Physica Medica 61 (2019) 8–17

Contents lists available at ScienceDirect

Physica Medica

journal homepage: www.elsevier.com/locate/ejmp

Original paper

Relative efficiency of Gafchromic EBT3 and MD-V3 films exposed to low-energy photons and its influence on the energy dependence

Guerda Massillon-JL*, Alexis Cabrera-Santiago, Nahum Xicohténcatl-Hernández

Instituto de Física, Universidad Nacional Autónoma de México, 04510 Coyoacan, Mexico City, Mexico

ARTICLE INFO

Keywords:
Low-energy-X-rays
Gafchromic-films
EBT3
MD-V3
^{60}Co-gamma
Monte-Carlo
Energy-dependence
Ionisation-density
Phantom material
Relative efficiency
Relative response
Intrinsic energy dependence
Track-average LET

ABSTRACT

Energy-dependence of Gafchromic films exposed to low-energy photons has been reported to be a function of absorbed-dose. However, these studies are based on a relative-response, *R*, which considers the absorbed-dose in water and not within the film sensitive-volume. This work investigated the relative-efficiency, RE_{film}, (ratio of absorbed-dose required to produce the same net optical density (netOD) by ^{60}Co gamma and by x-ray) of Gafchromic EBT3 and MD-V3 films exposed to five x-ray beams from 20 kV to 160 kV and ^{60}Co gamma rays. A factor that accounts for the energy-dependence, $f_{x,Q,med}$, based on RE_{film}, phantom-material and depth at which the films are placed during irradiation was used to remove the influence of absorbed dose. Values of RE_{film} indicated that the absorbed dose from ^{60}Co gamma rays needs to be 4 and 3 times larger than those from 20 kV x-rays to produce the same netOD within the EBT3 and MD-V3 sensitive volumes, respectively. Thus, saturation could help explain why Gafchromic films show under-response to very low doses from low-energy photon beams, regardless of film model. Furthermore, RE_{film}, was found to be nearly independent of netOD and colour-channels. Consequently, $f_{x,Q,med}$ is independent of the absorbed dose and colour-channels. In contrast, besides the variation with the photon energy, $f_{x,Q,med}$ varied with film model, depth and phantom material used during the irradiation. Thus, the results suggest that $f_{x,Q,med}$ is a more reliable wide-ranging parameter for evaluating the degree of energy-dependence of the film rather than the relative-response method commonly considered.

1. Introduction

Low-energy photons interact with matter liberating 'primary electrons' which generate low-energy 'secondary electron' (SE) cascades along their tracks through elastic and inelastic collisions. Recent results have indicated that most SEs generated by low-energy x-rays have kinetic energy below 10 keV, whose corresponding track-average linear energy transfer (LET) in LiF:Mg, Ti and liquid water are around 19 keVμm^{-1} and 9 keV μm^{-1}, respectively [1]. This suggested that low-energy x-rays could be considered as nearly high-ionization density radiation (HIDR). Usually, the effects induced by HIDR in physics or biological systems are scrutinized in terms of a parameter called relative efficiency or relative effectiveness, *RE*. In physical systems, *RE* is defined as the response per absorbed dose unit (within the sensitive volume of the system) induced by HIDR with respect to the same quantity by a reference field considered as low-ionization density (LIDR) (e.g. ^{60}Co gamma) [2]. While within the biological framework, this parameter is defined as the ratio of the absorbed dose deposited by LIDR with respect to that imparted by HIDR that produces the same response.

Research about the response of several Gafchromic film models exposed to low–energy x-rays has been published in the literature where under and/or over-response at energies below 100 keV relative to high energy photons (e.g. ^{60}Co gamma) are generally observed, regardless of the film model [3–18]. In order to develop new prototypes with more uniform energy response at low photon energies, the effects of varying the active layer composition of EBT GafChromic films have been investigated [18]. However, despite of all the improvements, up to 20% and 22% under-responses were still observed at 20 keV for the EBT3 films containing 7% Al and 4% Cl, respectively [18]. This suggests that understanding of low-energy radiation interaction with matter remains a challenge [1]. In addition, the degree of energy dependence of the film's response after exposure to low photon energies has been constantly reported to be a function of absorbed dose or air-kerma regardless of film model, mainly at low values of absorbed dose or air-kerma [3–4,12–14,16]. However, it is important to point out that in all these studies, the energy dependence of films has been analysed in terms of a relative response, *R*, defined as the film response per unit absorbed dose in water for a given photon energy beam relative to that for ^{60}Co gamma or 6 MV x-rays. This means that the absorbed dose

* Corresponding author.
E-mail address: massillon@fisica.unam.mx (G. Massillon-JL).

https://doi.org/10.1016/j.ejmp.2019.04.007
Received 17 October 2018; Received in revised form 10 April 2019; Accepted 11 April 2019
Available online 17 April 2019

within the film sensitive volume is not taken into account.

Richter and colleagues [16] tried to reduce the influence of the absorbed dose on the energy dependence of Gafchromic films by proposing a scaling factor that depended only on the beam energy and determined with the least squares method. Nonetheless, it was concluded that such factor could only be evaluated in energy beams where the photon attenuation in the film material is negligible [16] and, therefore, the results could not be directly transferred to other groups. According to Lindsay and colleagues [12], there exists a slight trend for increasing the film relative response, *R*, as a function of dose which, they assumed can be approximated by a first order exponential relationship with a constant that describes the amount of polymerization per unit dose. However, their report did not provide experimental evidence to support that statement. In contrast to their hypothesis, increasing and/or decreasing trend of the film relative response with dose have been observed, depending on the photon energy for a given batch of EBT2 or EBT3 films [13,14]. Thus, the investigation about a robust method based on relative efficiency, *RE,* instead of relative response, *R*, to determine the energy dependence of Gafchromic films that eliminates the influence of the absorbed dose is greatly necessary. This is because any variation on the absorbed dose could possibly affect the energy dependence factor. Results of such study might have an impact on the discrepancies reported by different groups about the degree of energy dependence of a given film model.

In this work, the relative efficiency, RE_{Film}, of Gafchromic EBT3 and MD-V3 films exposed to five x-ray beams from 20 kV to 160 kV and ^{60}Co gamma has been investigated considering a biological approach. In particular, an energy dependence factor, $f_{x,Q,med}$, based on *RE* has been defined in order to reduce the energy dependence of the absorbed dose. Besides, the phantom material and the depth at which the films are placed during the irradiation are also considered.

2. Methods

2.1. Preparation, readout and irradiation of the Gafchromic films

Three 1.4 × 1.4 cm^2 pieces of EBT3 and MD-V3 films were used at different absorbed dose levels. The EBT3 and MD-V3 films belonged to batch numbers 07221301 and A03051201, respectively. Fig. 1 displays the structure of both films and Table 1 presents the chemical compositions. The films were exposed in air to eight air kerma values between 0.1 Gy and 15.0 Gy from five x-ray beams (20 kV − 160 kV) (see Table 2a) generated by an YXLON Y.SMART 160E/1.5 x-ray tube installed in our lab at the UNAM Physics Institute. Fig. 2 shows several film pieces suspended in air with adhesive tape from a styrofoam frame during the x-ray irradiations. More details about the irradiation setup and how the x-ray beams were calibrated can be found in our previous report [14]. All film pieces were situated within a homogeneous circular radiation field of 8.2 cm diameter at 61 cm from the source focal spot (source to film distance: SFD). For these x-ray beams, a 61 cm air distance from the source was considered enough to provide charged particle equilibrium (CPE). The combined standard uncertainty (coverage factor $k = 1$) [19] on the delivered air kerma to the film was less than 0.5% and included the uncertainty from film placement, exposure time, thermometer, barometer and the ionization chamber calibration coefficient. For the ^{60}Co gamma irradiation, we used the reference beam from the National Institute of Standard and Technology (NIST) for absorbed dose in water ranging from 0.1 Gy to 15 Gy [14]. The films were positioned within a 14 × 14 cm^2 field size at 100 cm SFD in an acrylic phantom of 30 cm × 30 cm × 14 cm at 4.323 cm depth in order to provide CPE. For the air kerma delivered to the film in the absence of the acrylic phantom in the reference beam, the absorbed dose was divided by a conversion factor of 1.0899. This factor is the ratio of absorbed dose rate in water relative to the air kerma rate measured previously with the same ionization chamber under the same geometric conditions. The films were cut at least 48 h prior irradiation and read twenty-four hours post-irradiation. The reading process was carried out in transmission mode in an Epson Expression 11000XL document scanner at 300 dpi and 48 bit-RGB colour depths following the protocol established in our dosimetry laboratory [14,20]. The analysis of the film response was done using ImageJ software [21] by selecting a region of interest of 1.0 × 1.0 cm^2. The evaluation of the film response as well as the analysis of uncertainty were performed according to the methods described elsewhere [14].

Table 1
Chemical composition of the films according to the manufacturer.

Element	MD-V3		EBT3	
	Active layer (%): Z_{eff} = 7.63	Overall (%): Z_{eff} = 6.68	Active layer (%): Z_{eff} = 7.46	Overall (%): Z_{eff} = 6.71
H	58.20	38.30	56.50	38.40
Li	0.60	0.00	0.60	0.10
C	27.70	43.90	27.40	43.70
N	0.40	0.00	0.30	0.00
O	11.70	17.70	13.30	17.70
Na	0.50	0.00	0.10	0.00
Al	0.30	0.00	1.60	0.20
S	0.10	0.00	0.10	0.00
Cl	0.60	0.00	0.10	0.00

2.2. Evaluation of the relative efficiency, RE_{film}, of the films

The main requirement for evaluating *RE* in a physical system is that the response of such system with absorbed dose is linear. Thus, based on the fact that Gafchromic film response is not a linear function of the absorbed dose, the relative efficiency was evaluated experimentally and by Monte Carlo (MC) simulation similarly to biological system as follow:

2.2.1. Experiment

$$RE_{film} = \frac{D_{Film,Q_0}(netOD)}{D_{Film,Q}(netOD)}, \quad (1)$$

where $D_{Film,Q}(netOD)$ and $D_{Film,Q_0}(netOD)$ are the absorbed dose delivered within the film sensitive volume during the irradiation by photon energy beams of quality Q and Q_0, respectively and required to activate the same amount of film colour centres, i.e. to produce the same netOD value. The beam quality Q_0 corresponds to ^{60}Co gamma rays.

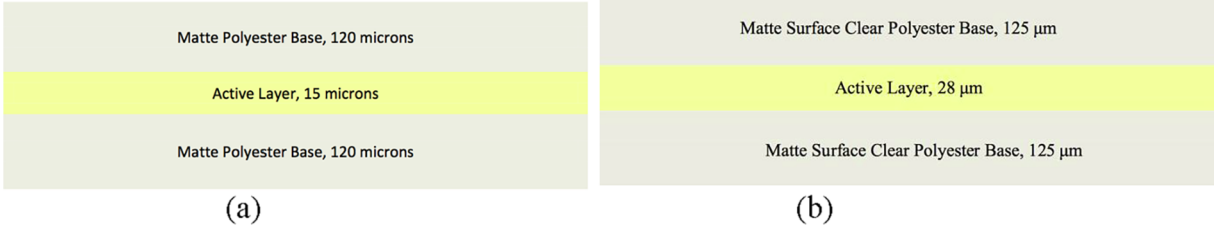

Fig. 1. Structure of the Gafchromic films according to the manufacturer: (a): MD-V3; (b): EBT3.

Table 2a
Characteristics of the x-ray beam qualities used in this work, the effective and average energy. Correction factor, f_a, for both films and the average mass-energy absorption ratios for different medium were obtained using the x-ray spectra produced by the SpekCal computer code [25]. These data are used to calculate the dose within the film sensitive volume.

Beam kV	HVL	*Effective Energy (keV)*	*Average energy (keV)*	f_a		$\left(\frac{\bar{\mu}_{en}}{\rho}\right)_{air}^{film}$		$\left(\frac{\bar{\mu}_{en}}{\rho}\right)_{air}^{water}$
	Al (mm)			*EBT3*	*MD-V3*	*EBT3*	*MD-V3*	
20	0.25 ± 0.19	13.48 ± 0.01	14.13	0.9581	0.9621	0.3779	0.3667	1.0227
50	1.13 ± 0.11	23.56 ± 0.04	28.53	0.9887	0.9899	0.4541	0.4476	1.0145
80	2.832 ± 0.11	32.33 ± 0.04	42.70	0.9940	0.9947	0.5978	0.5941	1.0252
120	6.538 ± 0.10	47.93 ± 0.02	60.23	0.9957	0.9963	0.8489	0.8506	1.0454
160	10.4 ± 0.23	67.39 ± 0.01	82.06	0.9962	0.9967	1.0850	1.0929	1.0628
^{60}Co			1250	1.000	1.000	1.5595	1.5775	1.1122

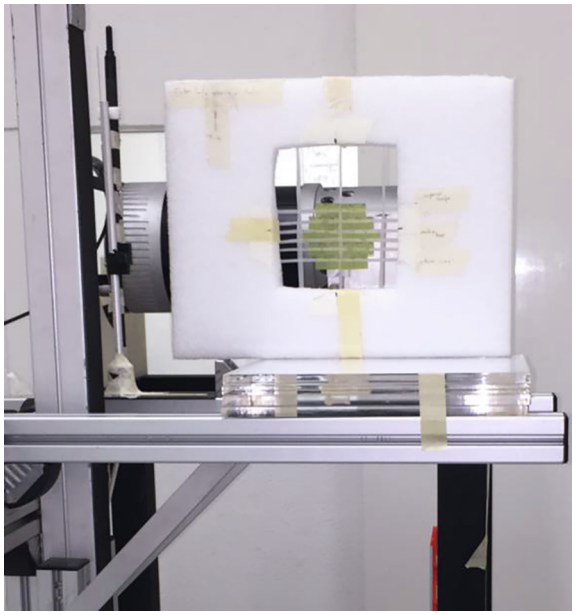

Fig. 2. Film irradiation setup in the x-ray beams.

2.2.2. MC simulation

MC simulation is based on the linearity of the detector response, that is the film response should be directly proportional to the absorbed dose. Then, to correct for the non-linearity of the film response with absorbed dose, we have applied a correction based on the exposure air kerma necessary to produce the same optical density from different energy photon beams as indicated in Eq. (2) below:

$$RE_{Film} = \frac{\left[\frac{D_{Film_{MC}}}{K_{air_{MC}}}.\ K_{air_{me}}(netOD)\right]_{Q_0}}{\left[\frac{D_{Film\,MC}}{K_{air_{MC}}}.\ K_{air_{me}}(netOD)\right]_{Q}}, \tag{2}$$

where $K_{air_{MC}}$and $K_{air_{me}}(netOD)$ are the air kerma calculated through the Monte Carlo simulation and measured with ionization chamber necessary to generate the same netOD from both beam qualities, respectively. $D_{Film_{MC}}$ is the absorbed dose within the sensitive volume of the film obtained with MC simulation.

The absorbed dose, $D_{Film_{MC}}$, and the air kerma, $K_{air_{MC}}$, were calculated through MC simulation using the DOSRZnrc module from EGSnrc code [22] following the procedures described previously [1,23]. The simulation was carried out using the same geometry as that in a recently reported x-ray experiment [14]. That is, the film was situated in air at 61 cm source to film distance and in 8.2 cm diameter field size. For the ^{60}Co gamma measurements, the experimental setup mentioned above in section 2.1 was simulated. The parameters used in our previous work [1] were considered for the absorbed dose and the air kerma calculation. In these simulations, 5×10^9 histories were followed for the absorbed dose and 5×10^8 histories for the air kerma.

The experimental absorbed dose within the film sensitive volume for a beam quality Q was calculated following the AAPM TG-61 protocol [24], but corrected for the low-energy photon beam attenuation within the film base material, f_a, [23] through the following relation:

$$D_{Film,Q} = K_{air_{me}} f_a \left(\frac{\bar{\mu}_{en}}{\rho}\right)_{air}^{Film} = K_{air} f_a \frac{\int_0^{E_{max}} \left(\frac{\mu_{en}(E)}{\rho}\right)_{Film} E\Phi(E)dE}{\int_0^{E_{max}} \left(\frac{\mu_{en}(E)}{\rho}\right)_{Air} E\Phi(E)dE}, \tag{3}$$

where

$$f_a = \frac{\int_0^{Emax} \Phi(E)\left(\frac{\mu_{en}(E)}{\rho}\right)_{Film} exp\left[-\left(\frac{\mu(E)}{\rho}\right).\rho x\right]_{Polyester} exp\left[-\left(\frac{\mu(E)}{\rho}\right).\rho x\right]_{Film} EdE}{\int_0^{Emax} \left(\frac{\mu_{en}(E)}{\rho}\right)_{Film} E\Phi(E)dE}$$

where $K_{air,me}$ is the measured air kerma, f_a is a correction factor that accounts for the average deposited energy by the photon beam within the film sensitive volume; *polyester* is the film base material and x the layer thickness of each region; $\Phi(E)$ is the photon fluence of energy E calculated using the SpekCalc computational code [25] and shown in Fig. 3. $\mu_{en}/\rho(E)$ and $\mu/\rho(E)$ are the mass-energy absorption and the mass-attenuation coefficients, respectively obtained from the XCOM database publicly available on the NIST website [26] and Fig. 4 displays the mass-energy absorption coefficients calculated based on the data in Table 1.

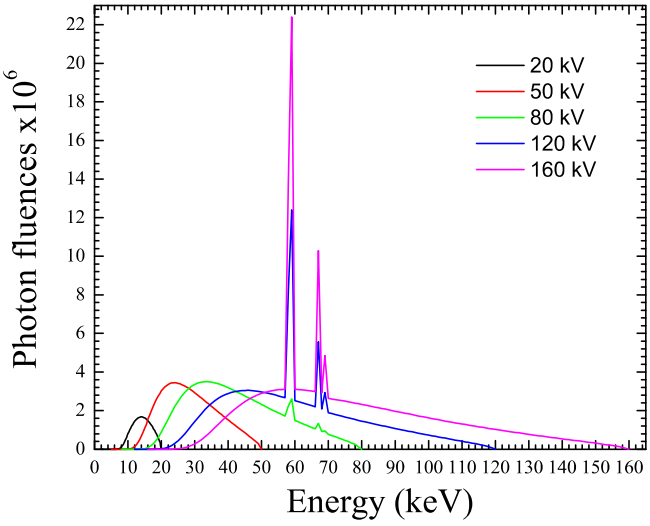

Fig. 3. X-ray spectra obtained with the SpekCal program and used for the absorbed dose calculations.

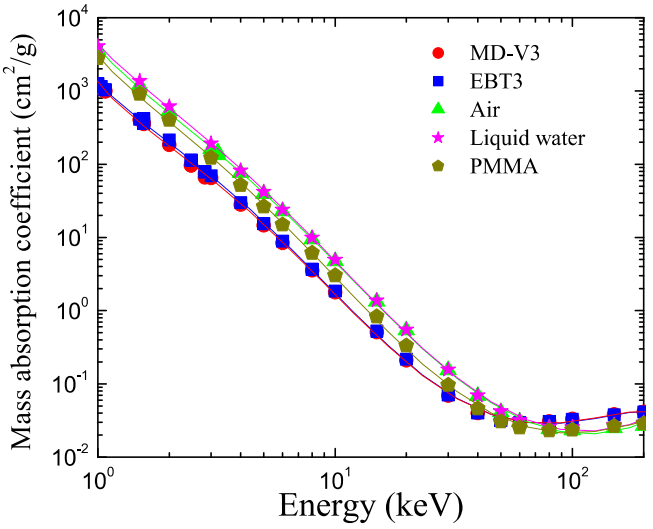

Fig. 4. Mass absorption coefficient calculated for the film sensitive volume based on data shown in Table 1. Also include data for air, liquid water and PMMA.

2.3. Evaluation of the energy dependence factor, $f_{x,Q,med}$, of the films

From a practical point of view, as the film is generally exposed at a given depth, *x*, of a given phantom material of medium, *med*, the factor that accounts for the energy dependence for a beam quality *Q*, $f_{x,Q,med}$, can be evaluated by the following relation:

$$f_{x,Q,med} = \frac{D_{x,med,Q}(netOD)}{D_{x,med,Q_0}(netOD)}, \tag{4}$$

where,

$$\frac{D_{x,med,Q}(netOD)}{D_{x,med,Q_0}(netOD)} = \frac{D_{Film,Q}(netOD)}{D_{Film,Q_0}(netOD)} \frac{\left[\frac{\int_0^{Emax}\Phi(E)\left(\frac{\mu_{en}(E)}{\rho}\right)_{med} exp\left[-\left(\frac{\mu(E)}{\rho}\right).\rho x\right]_{med} EdE}{\int_0^{Emax}\left(\frac{\mu_{en}(E)}{\rho}\right)_{Film} E\Phi(E)dE}\right]_Q}{\left[\frac{\int_0^{Emax}\Phi(E)\left(\frac{\mu_{en}(E)}{\rho}\right)_{med} exp\left[-\left(\frac{\mu(E)}{\rho}\right).\rho x\right]_{med} EdE}{\int_0^{Emax}\left(\frac{\mu_{en}(E)}{\rho}\right)_{Film} E\Phi(E)dE}\right]_{Q_0}} \tag{5}$$

Then Eq. (4) becomes:

$$f_{x,Q,med} = \frac{1}{RE_{film}} \cdot \frac{\left[\frac{\int_0^{Emax}\Phi(E)\left(\frac{\mu_{en}(E)}{\rho}\right)_{med} exp\left[-\left(\frac{\mu(E)}{\rho}\right).\rho x\right]_{med} EdE}{\int_0^{Emax}\left(\frac{\mu_{en}(E)}{\rho}\right)_{Film} E\Phi(E)dE}\right]_Q}{\left[\frac{\int_0^{Emax}\Phi(E)\left(\frac{\mu_{en}(E)}{\rho}\right)_{med} exp\left[-\left(\frac{\mu(E)}{\rho}\right).\rho x\right]_{med} EdE}{\int_0^{Emax}\left(\frac{\mu_{en}(E)}{\rho}\right)_{Film} E\Phi(E)dE}\right]_{Q_0}} \tag{6}$$

For measurements where the dosimeter is situated at the entrance surface of the phantom material, Eq. (6) becomes:

$$f_{0,Q,med} = \frac{1}{RE_{film}} \cdot \frac{\left[\left(\frac{\bar{\mu}_{en}}{\rho}\right)_{film}^{med}\right]_Q}{\left[\left(\frac{\bar{\mu}_{en}}{\rho}\right)_{film}^{med}\right]_{Q_0}}, \tag{7}$$

Table 2b presents the average mass-energy absorption coefficient ratios for air, liquid water and polymethyl methacrylate (PMMA) calculated using the x-ray spectra produced by the SpekCal computer code [25].

Eqs. (6) and (7) are based on the fact that the amount of ionization density produced by a given photon energy beam depends on the phantom material used during irradiation of the film [23], which can influence the energy dependence [10,23]. From these equations, it assumes that any contribution of backscatter radiation should be reflected on the film response relative efficiency, RE_{film}.

Table 2b
Average mass-energy absorption ratios for different medium obtained using the x-ray spectra produced by the SpekCal computer code [25]. These data were used to calculate the energy dependence factor.

Beam kV	*Effective Energy (keV)*	$\left(\frac{\bar{\mu}_{en}}{\rho}\right)_{film}^{Air}$		$\left(\frac{\bar{\mu}_{en}}{\rho}\right)_{film}^{water}$		$\left(\frac{\bar{\mu}_{en}}{\rho}\right)_{film}^{PMMA}$	
		EBT3	*MD-V3*	*EBT3*	*MD-V3*	*EBT3*	*MD-V3*
20	13.48 ± 0.01	2.6465	2.7267	2.7066	2.7887	1.6206	1.6697
50	23.56 ± 0.04	2.2023	2.2343	2.2343	2.2668	1.3839	1.4041
80	32.33 ± 0.04	1.6729	1.6832	1.7151	1.7256	1.1507	1.1577
120	47.93 ± 0.02	1.1780	1.1757	1.2315	1.2290	0.9298	0.9280
160	67.39 ± 0.01	0.9216	0.9150	0.9795	0.9725	0.8105	0.8047
^{60}Co	1250	0.6412	0.6339	0.7131	0.7050	0.6932	0.6853

3. Results

The netOD as a function of the absorbed dose within the film sensitive volume is displayed in Figs. 5a and 5b for the EBT3 and MD-V3, respectively. The symbols are the experimental data and the lines correspond to a polynomial fit to data. Independent of the film models and for a given absorbed dose value, the netOD increases as the photon energy beam decreases, which is possibly associated to the high pattern of energy deposited within the film by low energy secondary electrons generated by the photons. Tables 3a and 3b present the absorbed dose within the film sensitive volume for three netOD values of all the colour channels as a function of the photon energy beam. Note that the absorbed dose associated to a given netOD value (corresponding to each colour channel) increases with photon energy, regardless of film model. Also, Tables 3a and 3b show that, within measurement uncertainty, the absorbed dose does not depend on the colour channels. Therefore, a weight averaged relative efficiency of the three colour channels, RE_{Film}, for three netOD values evaluated with Eqs. (1) and (2) was obtained and is shown in Figs. 6a and 6b for both film models. Besides the colour channels, RE_{Film} also appears to be independent of netOD within measurement uncertainties. Thus, a weight averaged RE_{Film} was obtained for the three netOD values as a function of the photon energy beam. Table 4 displays the result and note that the relative efficiency for the MD-V3 film has higher uncertainty than the EBT3 film. This is due to the dose interval considered in this study (0.1 Gy and 15.0 Gy). It is well known that the optimum absorbed dose limits for the MD-V3 and EBT3 films are around 25 Gy [20,28] and 10 Gy [14], respectively. Qualitative agreement can be seen between the Monte Carlo simulation and the experiment. In both cases RE_{Film} increases as the photon energy decreases, which means that higher absorbed dose is required from high photon energy beam in order to produce the same response within the film sensitive volume at low energy. Fig. 7a shows the energy dependence factors, $f_{x,Q,med}$, calculated with Eq. (6) using data from Tables 2b and 4 for both film models as a function of depth in the PMMA phantom. A rapid decrease of $f_{x,Q,med}$ with depth can be observed, as well as a decrease in the $f_{x,Q,med}$ as the photon energy decreases. Table 5 and Fig. 7b show $f_{0,Q,med}$ as a function of the effective energy, considering measurements performed in air and at the entrance surface of liquid water and PMMA phantom material, i.e. at a depth $x = 0$. A clear influence of the phantom material is observed, independent of the film models and a larger energy dependence can be observed for the MD-V3 film. Also shown in Fig. 7b are the relative total energy dependence for EBT3 reported in the literature [9,18] and a qualitative agreement can be seen.

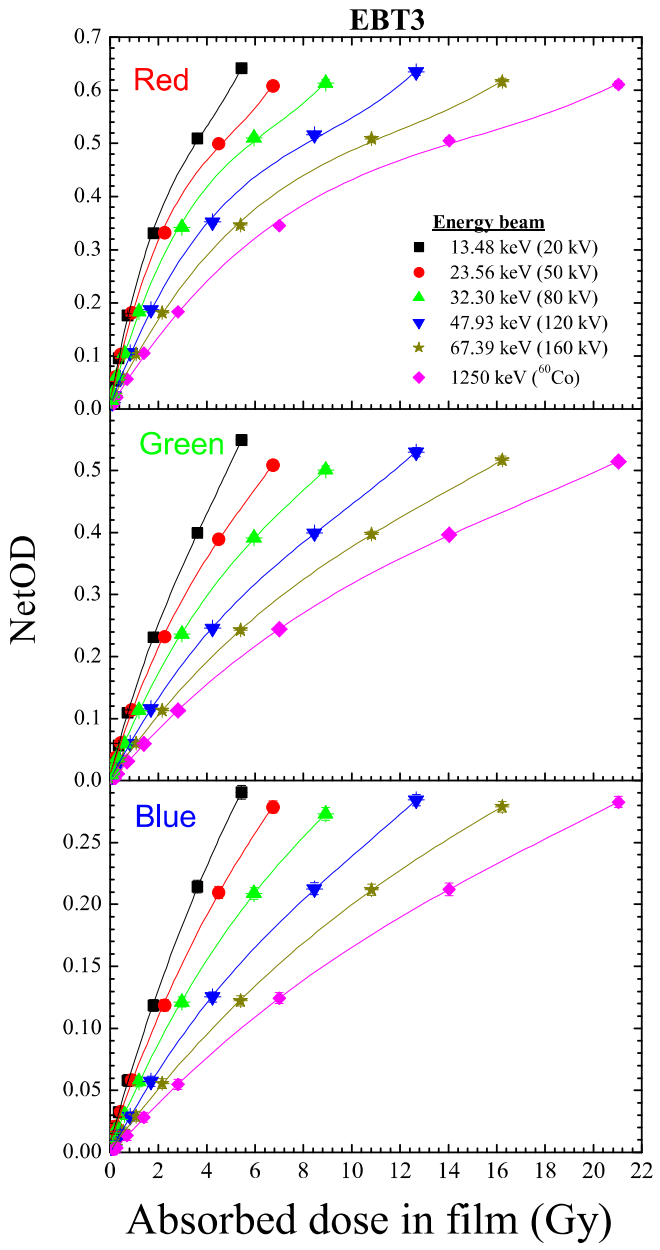

Fig. 5a. NetOD as a function of the absorbed dose (calculated with Eq. (1)) within the EBT3 film sensitive volume.

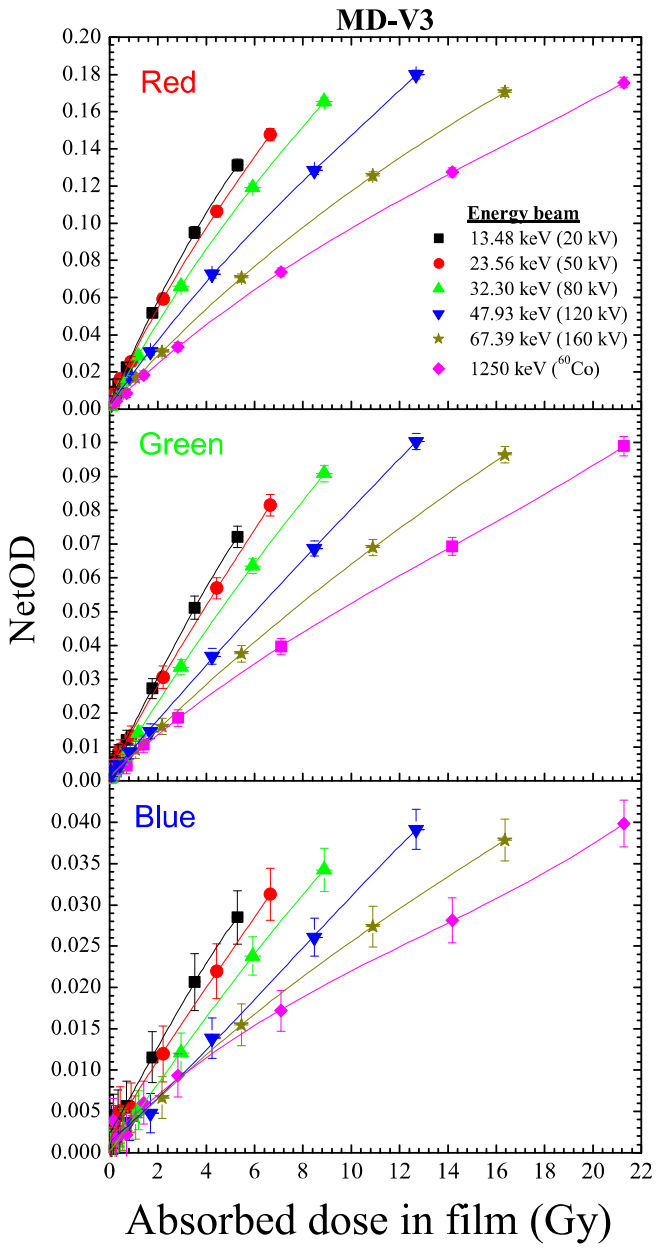

Fig. 5b. NetOD as a function of the absorbed dose (calculated with Eq. (1)) within the MD-V3 film sensitive volume.

4. Discussion

This work investigated the relative efficiency, *RE,* of Gafchromic EBT3 and MD-V3 films exposed to five x-ray beams from 20 kV to 160 kV and ^{60}Co gamma to determine its influence on the energy dependence factor, $f_{x,Q,med}$, in order to reduce the influence of absorbed dose and colour channel. As observed in Figs. 5a and 5b, the netOD is nearly constant (variation around 0.44% versus 1.12% maximum uncertainty) for several absorbed dose values, independent of film models and colour channel. This is particularly interesting since even at very low netOD values (i.e. low dose delivered), such a feature is still observed.

4.1. Relative efficiency, RE_{film}, of the films

According to Figs. 6a and b, within uncertainties, the relative efficiency, RE_{Film}, increases with decreasing photon energy beams, independent of the film models and netOD values for both Monte Carlo and experimental methods. This implies that much lower absorbed dose needs to be delivered by low photon energy than high energy beam in order to activate the same amount of colour centers within the film sensitive volume. This is due to the very compressed ionization density distribution generated by secondary electrons from low photon energies relative to that created by a high photon energy beam which is sparsely imparted. The results also suggest that the activation of colour centres that gives rise to the polymerization process might probably be governed by the amount of ionization density, i.e. LET, produced by a given beam quality regardless of the amount of absorbed dose delivered during the irradiation process. For example, both experiment and Monte Carlo results suggest that roughly 3.8–3.2 and 2.7–2.2 times more absorbed dose delivered by ^{60}Co gamma rays are required to produce the same response in EBT3 and MD-V3, respectively, than when exposed to 20 kV x-rays. This means that, regardless of the absorbed dose delivered during the irradiation, the film response will be raised with decreasing photon energy up to the limit that all colour centres are fully activated and reach saturation. Comparing the relative

Table 3a
Absorbed dose in EBT3 film for three netOD values as a function of colour channel and photon energy. Combined standard uncertainty corresponds to 1σ (coverage factor $k = 1$) [19].

EBT3									
	Red			Green			Blue		
netOD	0.5099 ± 0.0057	0.1758 ± 0.0038	0.0533 ± 0.0035	0.3990 ± 0.0055	0.1097 ± 0.0038	0.0331 ± 0.0035	0.2142 ± 0.0051	0.0580 ± 0.0046	0.0191 ± 0.0045
Beams	Absorbed dose in film (Gy)			Absorbed dose in film (Gy)			Absorbed dose in film (Gy)		
20 kV	3.6200 ± 0.0134	0.7232 ± 0.0027	0.1802 ± 0.0007	3.6200 ± 0.0134	0.7232 ± 0.0027	0.1802 ± 0.0007	3.6200 ± 0.0134	0.7232 ± 0.0027	0.1802 ± 0.0007
50 kV	4.7214 ± 0.1324	0.8743 ± 0.0284	0.2079 ± 0.0163	4.6807 ± 0.1216	0.876 ± 0.0376	0.2110 ± 0.0281	4.6630 ± 0.1714	0.9231 ± 0.0885	0.2151 ± 0.0782
80 kV	6.0328 ± 0.1573	1.1313 ± 0.0338	0.2691 ± 0.0221	6.1750 ± 0.1507	1.1637 ± 0.0476	0.2896 ± 0.0380	6.2037 ± 0.2255	1.2375 ± 0.1122	0.333 ± 0.1006
120 kV	8.2139 ± 0.1889	1.5535 ± 0.0455	0.3891 ± 0.0275	8.3788 ± 0.1769	1.5828 ± 0.0646	0.4308 ± 0.0471	8.5381 ± 0.2850	1.7204 ± 0.1513	0.5406 ± 0.1251
160 kV	10.9118 ± 0.2547	2.0554 ± 0.0575	0.5211 ± 0.0383	10.8630 ± 0.2322	2.0762 ± 0.0829	0.5513 ± 0.0648	11.0245 ± 0.1781	2.2964 ± 0.1984	0.6921 ± 0.1781
^{60}Co	14.3344 ± 0.3347	2.6276 ± 0.0733	0.6915 ± 0.0473	14.1303 ± 0.3000	2.6801 ± 0.1050	0.7736 ± 0.0795	14.1753 ± 0.4678	2.9519 ± 0.2505	0.9671 ± 0.2145

Table 3b
Absorbed dose in MD-V3 film for three netOD values as a function of colour channel and photon energy. Combined standard uncertainty corresponds to 1σ (coverage factor $k = 1$) [19].

MD-V3									
	Red			Green			Blue		
netOD	0.0951 ± 0.0031	0.0226 ± 0.0026	0.0091 ± 0.0026	0.0512 ± 0.0034	0.0121 ± 0.0029	0.0058 ± 0.0027	0.0207 ± 0.0035	0.0056 ± 0.0030	0.0038 ± 0.0033
Beams	Absorbed dose in film (Gy)			Absorbed dose in film (Gy)			Absorbed dose in film (Gy)		
20 kV	3.5280 ± 0.0130	0.7048 ± 0.0026	0.1790 ± 0.0006	3.5280 ± 0.0130	0.7048 ± 0.0026	0.1790 ± 0.0006	3.5280 ± 0.0130	0.7048 ± 0.0026	0.1790 ± 0.0006
50 kV	3.8654 ± 0.1532	0.7397 ± 0.0989	0.2488 ± 0.0911	3.9126 ± 0.2901	0.7576 ± 0.2189	0.2975 ± 0.1998	4.0822 ± 0.8063	0.8241 ± 0.6050	0.4617 ± 0.6488
80 kV	4.5073 ± 0.1752	0.9259 ± 0.1134	0.3727 ± 0.1045	4.6630 ± 0.3353	1.0188 ± 0.2525	0.4883 ± 0.2303	5.1142 ± 0.9190	1.3267 ± 0.7191	0.8947 ± 0.7757
120 kV	5.8996 ± 0.2262	1.1732 ± 0.1539	0.4046 ± 0.1436	6.1643 ± 0.4320	1.2738 ± 0.3545	0.5234 ± 0.3283	6.6664 ± 1.1564	1.5686 ± 1.0375	0.9400 ± 1.1384
160 kV	7.7674 ± 0.3119	1.5073 ± 0.3119	0.5528 ± 0.1761	7.7175 ± 0.5818	1.5490 ± 0.4151	0.6814 ± 0.3747	7.7074 ± 1.5572	1.6928 ± 1.0574	1.0641 ± 1.1170
^{60}Co	9.7351 ± 0.3932	1.8533 ± 0.2430	0.6538 ± 0.2212	9.6758 ± 0.7451	1.7781 ± 0.5312	0.6678 ± 0.4795	9.0564 ± 1.9688	1.5355 ± 1.3034	0.7621 ± 1.3712

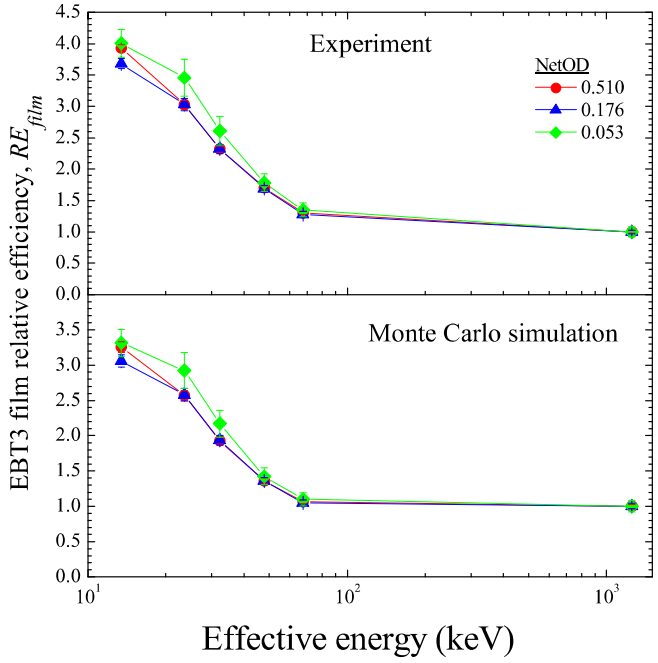

Fig. 6a. Weight averaged relative efficiency of the three colour channels, RE_{film}, for EBT3 film as a function of effective photon energy.

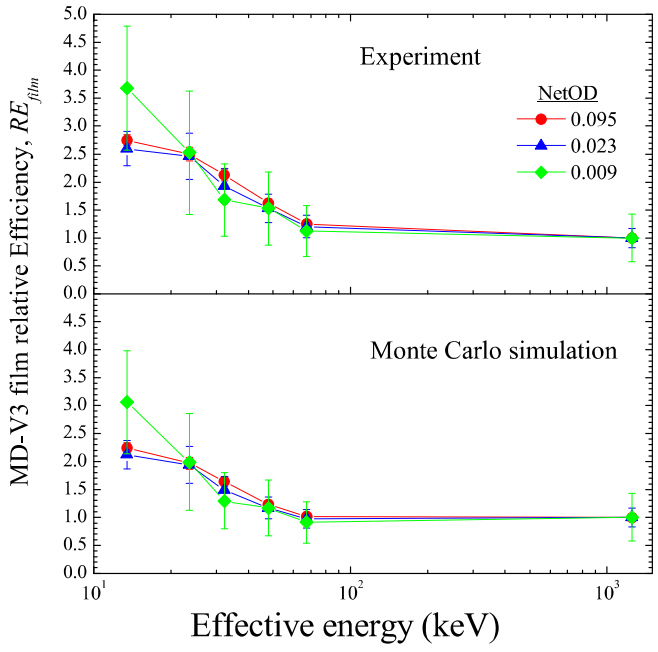

Fig. 6b. Weight averaged relative efficiency of the three colour channels, RE_{film}, for MD-V3 film as a function of effective photon energy.

efficiency results (Figs. 6a and b), the Monte Carlo simulation reproduces qualitatively quite well the experimental data. However, quantitative differences of around 20% are observed for both film models, independent of the photon energy beam. Such differences were expected and supported by our previous analysis of the thermoluminescent response of LiF;Mg,Ti exposed to 20–300 kV narrow x-ray spectra, ^{137}Cs and ^{60}Co [23] which, were associated to the non-existent of accurate cross sections for electron interactions at energies below 1 keV in the MC code [23,27].

For a similar film area of 1.4 × 1.4 cm^2 analysed in this work, the sensitive volume of EBT3 film is roughly twice that of MD-V3 (see Fig. 1). However, data in Table 4 indicate that RE_{film} for EBT3 film are greater than those for MD-V3 by only by 29% to 4%, being smaller at high energy. Nevertheless, if RE_{film} is normalized with respect to the active layer, an inverse scenario is observed. That is, RE_{film} per micron for MD-V3 is greater than that obtained for EBT3 by about 24%–44%, being smaller at lower energy, regardless of the method used (experiment or Monte Carlo). The high efficiency of the MD-V3 film could be explained by the differences in the concentrations of chemical elements present in each film model as displayed in Table 1. The concentration of chlorine within the MD-V3 film sensitive volume is 6 times that of EBT3. Thus, being the chemical element with the larger atomic number, Z, the chlorine has a higher interaction probability with the photons, which would translate into more ionization density. This means that at low photon energy where the photoelectric is the most important effect with cross-section interaction proportional to Z^3, the RE_{film} increases and steadily decreases when the cross-section interaction becomes proportional to Z as the Compton effect is taking place.

On the other hand, it can be seen that the relative efficiency for the MD-V3 film has higher uncertainty than the EBT3 film. This is due to the dose interval considered in this study (0.1 Gy and 15.0 Gy). It is well known that the optimum absorbed dose limits for the MD-V3 and EBT3 films are around 25 Gy [20,28] and 10 Gy [14], respectively

4.2. Energy dependence factor, $f_{x,Q,med}$, of the films

As Fig. 7a indicates, the energy dependence factor, $f_{x,Q,med}$ strongly depends on depth and photon energy. At low photon energies, e.g. at 20 kV X-rays, $f_{x,Q,med}$ for both film models rapidly decreases and tends to zero at about 20 mm depth in PMMA. And as the photon energy increases, $f_{x,Q,med}$ diminishes gradually. $f_{x,Q,med}$ tends to zero can be interpreted as a result of the rapid decrease of the photon fluence with increasing phantom depth caused by the photoelectric effect at low-energies [23] and the slight change in the absorbed dose at energies where the Compton effect becomes dominant, i.e. at ^{60}Co gamma. Such feature should be considered when film is exposed at a certain depth in phantom material during exposure to low photon energy beams. Concerning the energy dependence factor at the phantom entrance surface, $f_{0,Q,med}$, i.e. at depth $x = 0$, shown in Fig. 7b, note that the shape of the curve depends on the film models. Regardless of the phantom material, $f_{0,Q,med}$ for MD-V3 steadily decreases with photon energy, reaches a minimum, increases and then decreases toward ^{60}Co gamma. In the case of the EBT3 film situated in air and at the entrance surface of liquid water phantom, $f_{0,Q,med}$ increases, reaches a first maximum, then decreases to a minimum, then increases before decreasing to ^{60}Co gamma. For EBT3 situated on top of PMMA phantom, $f_{0,Q,med}$ monotonically increases as the energy augments. The difference observed on the shape of the energy-$f_{0,Q,med}$ curves between air, liquid water and PMMA could presumably be related to the photon interaction processes as seen in Fig. 4 and Table 2b. Noted in Fig. 7b, the energy dependence factor for both films situated at the entrance surface of PMMA phantom is strongly dominated by the film response's relative efficiency, RE_{Film}, which could be attributed to the relative proximity in terms of chemical compositions (differences on mass-absorption coefficient of 62%–67%) between PMMA and the film sensitive volume. However, for the films in air and at liquid water entrance surface, the energy dependence factor is dominated by their mass-absorption coefficients which are more than 2.7 times that of the film sensitive volume (see Table 2b).

The results also indicate that, regardless of the film models, the amplitude of $f_{0,Q,med}$ depends on the phantom material used during the irradiation process. The smaller the electronic density of the phantom material is, the larger the $f_{0,Q,med}$. This means that materials with higher electronic density can generate more ionization during the interaction process that would consequently contribute to the absorbed dose deposited within the film sensitive volume. Considering the energy interval studied, $f_{0,Q,med}$ varies from 1.071 ± 0.013 to 1.128 ± 0.020, from 0.985 ± 0.012 and 1.057 ± 0.018 and from 0.607 ± 0.007 to 0.900 ± 0.015 when the EBT3 film is irradiated in air, at the entrance

Table 4
Weight averaged relative efficiency obtained for the experimental absorbed dose and that calculated by Monte Carlo simulation. Combined standard uncertainty corresponds to 1σ (coverage factor $k = 1$) [19].

Equivalent Energy	RE_{Film}			
	Experiment		Monte Carlo simulation	
(keV)	EBT3	MD-V3	EBT3	MD-V3
13.48 ± 0.01	3.852 ± 0.046	2.743 ± 0.093	3.181 ± 0.053	2.237 ± 0.085
23.56 ± 0.04	3.044 ± 0.055	2.497 ± 0.117	2.588 ± 0.054	1.965 ± 0.099
32.33 ± 0.04	2.329 ± 0.041	2.099 ± 0.097	1.943 ± 0.040	1.617 ± 0.080
47.93 ± 0.02	1.704 ± 0.028	1.614 ± 0.075	1.364 ± 0.028	1.228 ± 0.061
67.39 ± 0.01	1.299 ± 0.022	1.245 ± 0.059	1.060 ± 0.022	1.007 ± 0.051
1044.7	1.000 ± 0.016	1.000 ± 0.048	1.000 ± 0.023	1.000 ± 0.053

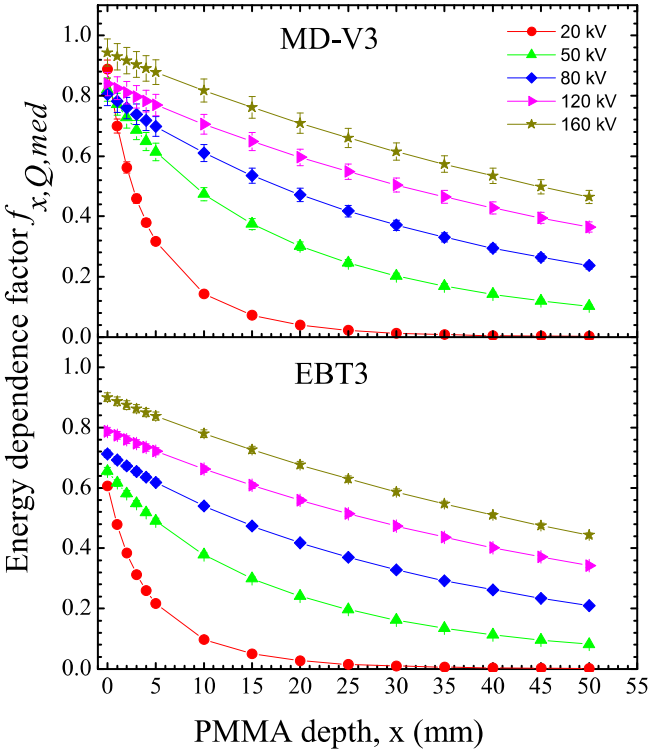

Fig. 7a. Energy dependence factor, $f_{x,Q,med}$, calculated with equation (5) as a function of the depth in PMMA for both films.

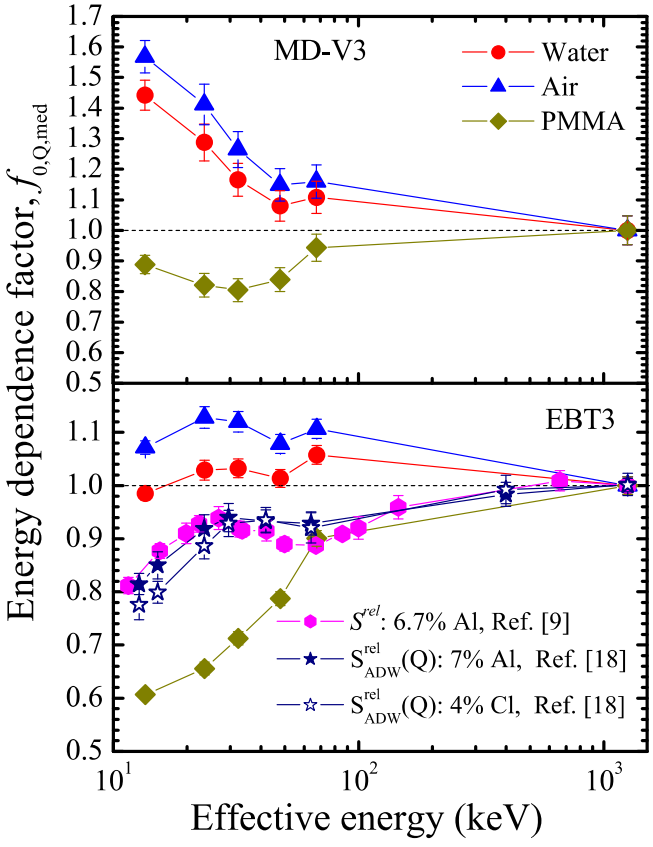

Fig. 7b. Energy dependence factor, $f_{0,Q,med}$, calculated with equation (6) as a function of the effective photon energy for both film models exposed in air and at the entrance surface of liquid water and PMMA phantom. Also shown, the relative response data published in the literature for EBT3 with 6.7% Al [9] as well as EBT3 with 7% Al and 4% Cl [18].

surface of liquid water and PMMA phantoms, respectively. While for MD-V3 situated in air, at the entrance surface of liquid water and PMMA phantoms, $f_{0,Q,med}$ fluctuates from 1.149 ± 0.053 to 1.568 ± 0.053, from 1.080 ± 0.050 to 1.442 ± 0.049 and from 0.805 ± 0.037 to 0.943 ± 0.045, respectively. As observed in Fig. 7b,

Table 5
Weight averaged energy dependence factor calculated with equation (7) for different medium. Combined standard uncertainty corresponds to 1σ (coverage factor $k = 1$) [19]: Experiment.

$f_{0,Q,med}$						
Equivalent Energy	Air		Liquid Water		PMMA	
(keV)	EBT3	MD-V3	EBT3	MD-V3	EBT3	MD-V3
13.48 ± 0.01	1.071 ± 0.013	1.568 ± 0.053	0.985 ± 0.012	1.442 ± 0.049	0.607 ± 0.007	0.888 ± 0.030
23.56 ± 0.04	1.128 ± 0.020	1.412 ± 0.066	1.029 ± 0.019	1.288 ± 0.061	0.656 ± 0.012	0.821 ± 0.039
32.33 ± 0.04	1.120 ± 0.019	1.265 ± 0.058	1.032 ± 0.018	1.166 ± 0.054	0.713 ± 0.012	0.805 ± 0.037
47.93 ± 0.02	1.078 ± 0.018	1.149 ± 0.053	1.013 ± 0.017	1.080 ± 0.050	0.787 ± 0.013	0.839 ± 0.039
67.39 ± 0.01	1.107 ± 0.018	1.159 ± 0.055	1.057 ± 0.018	1.108 ± 0.052	0.900 ± 0.015	0.943 ± 0.045
1044.7	1.000 ± 0.016	1.000 ± 0.048	1.000 ± 0.016	1.000 ± 0.048	1.000 ± 0.016	1.000 ± 0.048

MD-V3 is much more dependent on the photon energy than EBT3 and consequently, careful attention should be paid when used in radiation fields with important contributions of photon energies below 100 keV.

To compare the method proposed in this work with the "relative response" one commonly used by the community [4,12,14,16,18], the raw data obtained for the same EBT3 batch reported in Massillon-JL et al. [14] was reanalysed using the new method to determine the energy dependence factor. Besides being independent of absorbed dose and colour channel (results not shown), the results suggest that $f_{0,Q,med}$ is greater than the previous values. A variation of 2%–7% was previously reported for the red channel, which varied with the absorbed dose [14], versus 1.071 ± 0.013 to 1.128 ± 0.020 obtained in this work, depending on the photon energy beam. The result of this analysis suggests that the method used in the previous studies to convert the film response into absorbed dose is not correct, i.e. it is not appropriate to transform the absorbed dose in air to absorbed dose in water without considering the absorbed dose deposited within the sensitive volume of the film which generates the netOD. Thus, one can argue that $f_{x,Q,med}$ defined in this work is the most reliable parameter for evaluating the degree of energy dependence of the film rather than the method commonly used in the literature.

Fig. 7b also displays data reported in the literature for EBT3 which included 6.7% Al [9], 7% Al and 4% Cl [18]. Note that the relative total energy response, S^{rel} and $S^{rel}_{AD,w}(Q)$ described in Ref. [9] and Ref. [18], respectively, are very similar to the method commonly used by the community using a relative response, R. This method is based on the ratio of the film response per absorbed dose in water unit for a given beam quality Q with respect to the same for a reference radiation beam, Q_0. This means that this factor does not consider the absorbed dose deposited within the film sensitive volume. Nevertheless, qualitative agreement is still observed with our data, which should be associated to the physical interaction processes of photons with matter. Similar to $f_{0,Q,med}$ for EBT3 exposed in air and at the liquid water phantom entrance surface, the relative total energy responses, S^{rel} [9] and $S^{rel}_{AD,w}(Q)$ [18], increase, reach a first maximum, then decrease to a minimum, then increase before tending to ^{60}Co as the photon energies increase. However, at energies below 100 keV, discrepancies of around 9%-16% and 10%-21% are observed between $f_{0,Q,med}$ and, S^{rel} and $S^{rel}_{AD,w}(Q)$, respectively which agree with the result obtained for EBT3 film analysed through the relative response method and reported elsewhere [14]. Considering the small difference observed on $S^{rel}_{AD,w}(Q)$ between EBT3 with 7% Al and that containing 4% Cl [18], one can argue that the observed discrepancies are most likely related to the methods rather than the film batch and/or chemical composition. Consequently, $f_{0,Q,med}$ might be batch independent. In this case, more study should be performed with different film batches in order to confirm or not such assumption.

5. Conclusion

This work has investigated the relative efficiency, RE_{Film}, of Gafchromic EBT3 and MD-V3 films exposed to five x-ray beams from 20 kV to 160 kV and ^{60}Co gamma and its influence on the energy dependence. In particular, an energy dependence factor, $f_{x,Q,med}$, based on RE_{Film} has been determined in order to reduce the influence of the absorbed dose. The effect of phantom material and depth was also evaluated. The results suggest that higher absorbed dose is required from high photon energy beams in order to produce the same response within the film sensitive volume at low energy. Furthermore, within uncertainties, RE_{Film} and $f_{x,Q,med}$ were found to be independent of the absorbed dose and colour channel, but varied with film model, phantom material, depth and probably by ionization density. Thus, one can conclude that the $f_{x,Q,med}$, defined in this work, is the most reliable and wide-ranging parameter for evaluating the degree of energy dependence of Gafchromic films rather than the commonly used relative response, R. From a practical standpoint, this implies that for measurements performed in air, at the entrance surface of liquid water or PMMA phantom of the same film models exposed to photon beams within the energy range studied in this work, the data displayed in Tables 4 and 5 can be used through the interpolation method, otherwise Eqs. (1) and (6) should be applied.

Acknowledgments

The authors thank Profs. Maria Ester Brandan, Christy Holland and Ivan Rosado-Mendez for useful discussions, as well as Abel Hernandez-Guzman, Ivone Salas, Iván Domingo Muñoz-Molina, Eduardo López-Pineda and Cesar Gustavo Ruiz-Trejo for technical support. This work was partially supported by PAPIIT-UNAM grant IN115117 and Royal Society-Newton Advance Fellowship grant NA150212

References

[1] Cabrera-Santiago A, Massillon-JL G. Track-average LET of secondary electrons generated in LiF:Mg, Ti and liquid water by 20–300 kV x-ray, ^{13}7Cs and ^{6}0Co beams. Phys Med Biol 2016;61:7919–33.
[2] Hansen JW, Olsen KJ. Experimental and calculated response of a radiochromic dye film dosimeter to high-LET radiations. Radiat Res 1984;97:1–15.
[3] McCabe Bradley P, Speidel Michael A, Pike Tina L, Van Lysel Michael S. Calibration of GafChromic XR-RV3 radiochromic film for skin dose measurement using standardized x-ray spectra and a commercial flatbed scanner. Med Phys 2011;38:1919.
[4] Brown TAD, Hogstrom KR, Alvarez D, Matthews KLII, Ham K, Dugas JP. Dose–response curve of EBT, EBT2, and EBT3 radiochromic films to synchrotron-produced monochromatic x-ray beams. Med Phys 2012;39:7412–7.
[5] Butson MJ, Yu Peter KN, Tsang Cheung, Alnawaf H. Energy response of the new EBT2 radiochromic film to x-ray radiation. Radiat Meas 2010;45:836–9.
[6] Di Lillo F, Mettivier G, Sarno A, Tromba G, Tomic N, Devic S, et al. Energy dependent calibration of XR-QA2 radiochromic film. Med Phys 2016;43:583–8.
[7] Fletcher CL, Mills JA. An assessment of GafChromic film for measuring 50 kV and 100 kV percentage depth dose curves. Phys Med Biol 2008;53:N209–18.
[8] Giaddui T, Cui Y, Galvin J, Chen W, Yu Y, Xiao Y. Characteristics of Gafchromic XRQA2 films for kV image dose measurement. Med Phys 2012;39:842–50.
[9] Hammer CG, Rosen BS, Fagerstrom JM, Culberson WS, DeWerd LA. Experimental investigation of GafChromic EBT3 intrinsic energy dependence with kilovoltage x rays, ^{137}Cs, and ^{60}Co. Med Phys 2018;45:448–59.
[10] Hermida-López M, Lüdemann L, Flühs A, Brualla L. Influence of the phantom material on the absorbed-dose energy dependence of the EBT3 radiochromic film for photons in the energy range 3 keV–18 MeV. Med Phys 2014;41:112103–11.
[11] Khachonkham S, Dreindl R, Heilemann G, Lechner W, Fuchs H, Palmans H, et al. Characteristic of EBT-XD and EBT3 radiochromic film dosimetry for photon and proton beams. Phys Med Biol 2018;63:06500–6511.
[12] Lindsay P, Rink A, Ruschin M, Jaffray D. Investigation of energy dependence of EBT and EBT-2 Gafchromic film. Med Phys 2010;37:571–6.
[13] Massillon-JL G, Chiu-Tsao ST, Muñoz DI, Chan MF. Energy dependence of the new Gafchromic EBT3 film: dose response curves for 50 kV, 6 and 15 MV x-ray beams. Int J Med Phys Clin Eng Radiat Oncol 2012;1:60–5.
[14] Massillon-JL G, Muñoz-Molina ID, Díaz-Aguirre P. Optimum absorbed dose versus energy response of Gafchromic EBT2 and EBT3 films exposed to 20–160 kV x-rays and ^{60}Co gamma. Biomed Phys Eng Express 2016;2. 045005.
[15] Palmer AL, Jafari SM, Mone I, Muscat S. Evaluation and clinical implementation of in vivo dosimetry for kV radiotherapy using radiochromic film and micro-silica bead thermoluminescent detectors. Phys Med 2017;42:47–54.
[16] Richter C, Pawelke J, Karsch L, Woithe J. Energy dependence of EBT-1 radiochromic film response for photon 10 kVp–15 MVp and electron beams, 6–18 MeV readout by a flatbed scanner. Med Phys 2009;36:5506–14.
[17] Rink A, Vitkin IA, Jaffray D. A, Energy dependence (75 kVp to 18 MV) of radiochromic films assessed using a real-time optical dosimeter. Med Phys 2007;34:458–63.
[18] Bekerat H, Devic S, DeBlois F, Singh K, Sarfehnia A, Shih Seuntjens J, et al. Improving the energy response of external beam therapy (EBT) GafChromic dosimetry films at low energies (≤100 keV). Med Phys 2014;41. 022101-1-14.
[19] ANSI/NCSL Z540-2-1997 1997 US Guide to the Expression of Uncertainty in Measurement, American National Standard for Expressing Uncertainty (Boulder, CO: NCSL).
[20] Massillon-JL G, Zúñiga-Meneses L. The response of the new MD-V2-55 radiochromic film exposed to ^{60}Co gamma rays. Phys Med Biol 2010;55:5437–49.
[21] Image J 2017 (accessed July 2017).
[22] Kawrakow I, Mainegra-Hing E, Rogers DWO, Tessier F, Walters BRB, The EGSnrc Code System: Monte Carlo Simulation of Electron and Photon Transport NRCC PIRS-701 (Ottawa: National Research Council Canada, 2016).
[23] Massillon-JL G, Cabrera-Santiago A, Minniti R, O'Brien M, Soares C. Influence of phantom materials on the energy dependence of LiF:Mg, Ti thermoluminescence dosimeters exposed to 20–300 kV narrow x-ray spectra, ^{13}7Cs and ^{6}0Co photons. Phys Med Biol 2014;59:4149–66.
[24] Ma C-M, Coffey CW, DeWerd LA, Liu C, Nath R, Seltzer SM, et al. TG-61: AAPM protocol for 40–300 kV x-ray beam dosimetry in radiotherapy and radiobiology.

Med Phys 2001;28:868–93.
[25] Poludniowski G, Landry G, DeBlois F, Evans PM, Verhaegen F. *SpekCalc*: a program to calculate photon spectra from tungsten anode x-ray tubes. Phys Med Biol 2009;54:N433–8.
[26] Berger MJ, Hubbell JH, Seltzer SM, Chang J, Coursey JS, Sukumar R, et al. Database 1998. www.nist.gov/pml/data/xcom/index.cfm.
[27] Cabrera-Santiago A, Massillon-JL G. Secondary electron fluence generated in LiF:Mg, Ti by low-energy photons and its contribution to the absorbed dose. AIP Conf Proc 2016;1747:020004–20011.
[28] Massillon-JL G, Aragón-Martínez N, Gómez-Muñoz A, Hernández-Guzmán A. Absorbed dose to water rate in a Cyberknife VSI system reference field using ionization chambers and Gafchromic films. Int J Med Phys, Clin Eng Radiat Oncol 2017;6:80–92.